frontiers in Earth Science

ORIGINAL RESEARCH
published: 09 March 2022
doi: 10.3389/feart.2022.829300

Numerical Investigation on the Dynamic Evolution of Intra-Crustal Continental Delamination

Rui Qi[1], *Jie Liao*[1,2]*, *Xiaohui Liu*[1,2] *and Rui Gao*[1,2]*

[1]School of Earth Sciences and Engineering, Sun Yat-Sen University, Guangzhou, China, [2]Southern Marine Science and Engineering Guangdong Laboratory (Zhuhai), Zhuhai, China

Delamination often occurs in continental regions, through which process the lithospheric mantle detaches from the continental crust and sinks into the underlying asthenospheric mantle. Various modes of continental delamination are proposed, including the typical mode of delamination along the Moho and the newly proposed delamination along the mid-lithospheric discontinuity. Geological and geophysical observations reveal the possibility of an alternative mode of delamination, i.e., intra-crustal continental delamination, which is rarely studied. Using the 2D thermo-mechanical coupled geodynamical models, we systemically study the dynamic evolution of the intra-crustal continental delamination. Model results suggest that the intra-crustal continental delamination develops along the base of the upper crust, promoted by the intra-crustal decoupling, i.e., the mechanical strength decoupling between the upper and lower crust. The three physical parameters, i.e., the upper crustal thickness, the lower crustal rheology, and the initial Moho temperature all affect intra-crustal strength decoupling, and thus influence continental delamination. Combining with geological and geophysical observations, we speculate that intra-crustal continental delamination taking place along the upper and lower crustal interface is a possible way of continental destruction.

Keywords: intra-crustal continental delamination, crustal strength decoupling, geodynamical numeric modeling, intra-crustal decoupling, continental delamination

OPEN ACCESS

Edited by:
Zhong-Hai Li,
University of Chinese Academy of Sciences, China

Reviewed by:
Yujun Sun,
Chinese Academy of Geological Science, China
Huilin Wang,
Huazhong University of Science and Technology, China

***Correspondence:**
Jie Liao
liaojie5@mail.sysu.edu.cn
Rui Gao
gaorui66@mail.sysu.edu.cn

Specialty section:
This article was submitted to Structural Geology and Tectonics, a section of the journal Frontiers in Earth Science

Received: *05 December 2021*
Accepted: *24 January 2022*
Published: *09 March 2022*

Citation:
Qi R, Liao J, Liu X and Gao R (2022) Numerical Investigation on the Dynamic Evolution of Intra-Crustal Continental Delamination. Front. Earth Sci. 10:829300. doi: 10.3389/feart.2022.829300

INTRODUCTION

The destruction of continental lithosphere through delamination is often proposed. The critical conditions for the occurrence of delamination are density contrast (i.e., denser lithospheric mantle than the surrounding area) and a weak interface (Bird, 1978, 1979; Kay and Mahlburg Kay, 1993; Göğüş and Pysklywec, 2008; Faccenda et al., 2009; Burov, 2011; Krystopowicz and Currie, 2013; Magni et al., 2013; Göğüş et al., 2016; Beall et al., 2017; Göğüş and Ueda, 2018). The typical mode of continental delamination is that the relatively denser lithospheric mantle detaches and peels away from the overlying continental crust along the mechanically weak crust-mantle interface, i.e., the Moho (**Figure 1A**; Bird, 1978, Bird, 1979). Continental delamination along Moho is the most popular mode, and the proposed natural examples are the Western Mediterranean and the Eastern Anatolia (Göğüş and Pysklywec, 2008; Thurner et al., 2014). The previous geodynamical modeling studies have widely investigated this type of delamination and suggested that, for instance, a weak interface along Moho, low density of the lower crust, denser lithospheric mantle than the

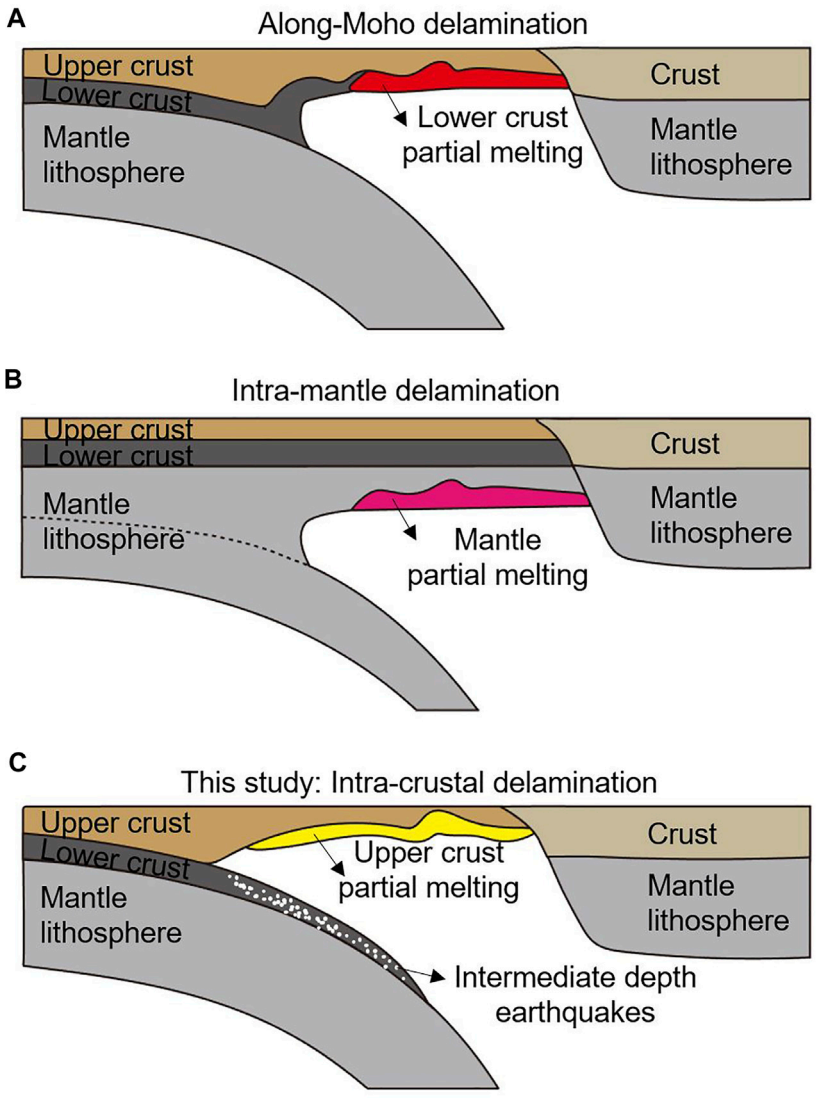

FIGURE 1 | Possible modes of continental delamination. **(A)** Along-Moho delamination. **(B)** Intra-mantle delamination. **(C)** The alternative mode of delamination: intra-crustal delamination. The earthquake data is from Fillerup et al. (2010).

asthenospheric mantle (Göğüş et al., 2016, 2011; Göğüş and Pysklywec, 2008; Li et al., 2016), low viscosity of the lower crust (Magni et al., 2013), and rapid upwelling of the partially molten mantle in the mantle wedge (Faccenda et al., 2009) are the key model parameters promoting delamination. However, in the regions where the lower crust is mechanically coupled with the underlying lithospheric mantle, the Moho may not represent a mechanical weak interface, and continental delamination may happen in different depth.

The recent studies proposed that continental delamination may happen in mid-lithospheric depth along a mid-lithospheric discontinuity (**Figure 1B**; Wang et al., 2018; Wang and Kusky, 2019). The intra-mantle delamination is proposed based on the North China Craton through geodynamical modeling (Wang et al., 2018). The modeling results indicated that the intra-mantle delamination needs smaller resultant stress and thus occurs relatively easier than that along Moho. Besides, the dynamics of intra-mantle delamination differs from the along-Moho delamination, since the former one may recycle larger amount of continental lithosphere into deep mantle (Wang et al., 2018).

The alternative scenario of delamination, termed as intra-crustal continental delamination (**Figure 1C**), is proposed in this study based on geological and geophysical observations which reveal decoupled deformation of the upper and lower crust (**Figure 2**). The possible natural examples of intra-crustal delamination are proposed in the Northern Apennines and in the southeast Carpathians (**Figure 2A**) based on the thin continental crust underneath the orogenic belt (i.e., due to the removal of the lower crust) and the subducting slabs with intermediate depth earthquakes possibly occurred in the

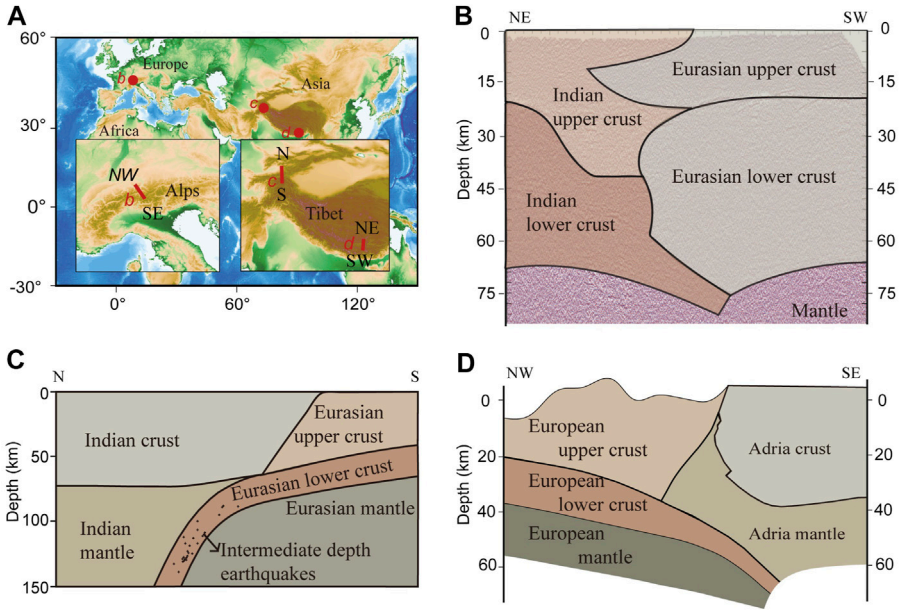

FIGURE 2 | Natural examples showing decoupled crustal deformation in collisional zones. **(A)** Locations of the Alpine orogen, the Northwestern and Southeastern Tibetan orogen. **(B–C)** Decoupled upper and lower crustal deformation in the Tibetan Plateau interpreted based on the deep seismic reflection data (Gao et al., 2016; Guo et al., 2017; Dong et al., 2020) and tele-seismic data (Schneider, 2013, 2019). **(D)** Decoupled upper and lower crustal deformation in the Alpine orogen (Schmid et al., 2017).

subducted lower crust (**Figure 1C**; Pauselli et al., 2006; Fillerup et al., 2010; Piana Agostinetti and Faccenna, 2018). Th e possibility of intra-crustal delamination is also supported by the widely observed intra-crustal decoupled crustal deformation (**Figure 2**). For instance, decoupled upper and lower crustal deformation is revealed by deep seismic reflection profiles in the central Himalayan Orogen (**Figures 2B,C**), where the lower crust of the Indian plate detached from the upper crust and subducted attached to the lithospheric mantle (Gao et al., 2016; Guo et al., 2017; Liang et al., 2018; Dong et al., 2020). This phenomenon is also observed in the Alpine orogeny (**Figure 2D**), where the upper crust detached from the lower crust during continental collision (Bousquet and Goff, 1997; Schmid et al., 2017). The possible reason of decoupled upper and lower crustal deformation is intra-crustal strength decoupling (Liao et al., 2017, 2018; Vogt et al., 2017, 2018), which may promote the intra-crustal delamination.

The intra-crustal delamination is a possible scenario, but its dynamic evolution remains poorly understood. In this study, we aim to systematically study the intra-crustal delamination using geodynamical numeric modeling, with specific attention paid on the influence of the controlling physical parameters. Model results are further discussed based on natural observations.

METHODS

Numerical Method

We use the thermomechanical coupled numerical code I2VIS (Gerya and Yuen, 2003, 2007) to simulate continental delamination following oceanic subduction. Assuming an incompressible media in a fully staggered grid, I2VIS uses the finite-differences and marker-in-cell techniques to solve the mass, momentum and energy conservation equations:

$$\frac{\partial v_i}{\partial x_i} = 0 \tag{1}$$

$$\frac{\partial \sigma'_{ij}}{\partial x_j} - \frac{\partial P_i}{\partial x_i} = -\rho g_i \tag{2}$$

$$\rho C_p\left(\frac{dT}{dt}\right) = \frac{\partial}{\partial x_i}\left(k\frac{\partial T}{\partial x_i}\right) + H_s + H_r + H_a + H_L \tag{3}$$

where v is velocity, σ' is the deviatoric stress tensor, P is the pressure, ρ is the density, g is the gravitational acceleration, C_p is the heat capacity, T is the temperature, k is the thermal conductivity. H_s is shear heating, H_a is the adiabatic heating, H_r is the radioactive heating with a constant value for each rock, and H_L is the latent heating included implicitly by increasing the effective heat capacity and thermal expansion of the partially crystallized/molten rocks (Burg and Gerya, 2005).

We employ visco-plastic rheology in our numerical models. The non-Newtonian viscous rheology (**Eq. 4**) depends on strain rate, pressure and temperature, where $\eta_{ductile}$ is the ductile viscosity, $\dot{\varepsilon}_{II}$ is the square root of the second invariant of strain rate, A_D is the Material constants, E is the activation energy, V is the activation volume, n is the power label of the deviatoric stress, these four parameters can be determined by the experimental petrology. Yield stress (σ_{yield}) is described by a Drucker-Prager yield criterion where C is the rock cohesion and μ is the effective friction coefficient, the yielding stress σ is only depend on pressure (P). Plastic viscosity

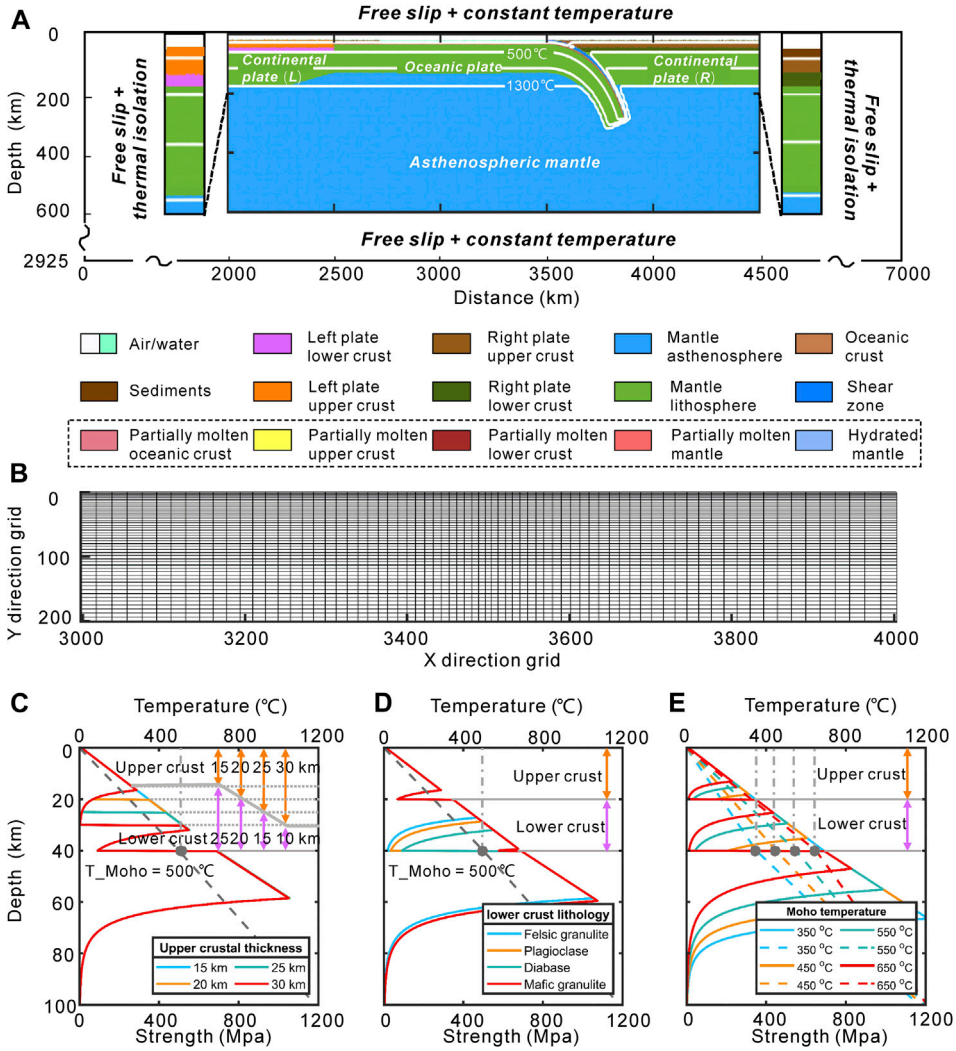

FIGURE 3 | Model setup. **(A)** Initial model configuration. A slab nose is initially imposed in the model to drive oceanic subduction. Colors in the dotted box are newly formed rocks. **(B)** Grid of a part of the model. **(C)** Lithospheric mantle strength with different crustal thickness. **(D)** Lithospheric mantle strength with different lower crustal lithology. **(E)** Lithospheric mantle strength with different Moho temperature.

($\eta_{plastic}$) is computed based on the square root of the second invariant of strain rate ($\dot{\varepsilon}_{II}$). The effective viscosity (η_{eff}) of rocks is the minimum of the ductile viscosity and plastic viscosity (Ranalli, 1995). See further explanation of variables/symbols in **Supplementary Table S1** in the supplement (Kirby and Kronenberg, 1987; Wilks and Carter, 1990; Clauser and Huenges, 1995; Ranalli, 1995; Turcotte and Schubert, 2002; Afonso and Ranalli, 2004).

$$\eta_{ductile} = (\dot{\varepsilon}_{II})^{\frac{1-n}{n}} (A_D)^{-\frac{1}{n}} exp\left(\frac{E+PV}{nRT}\right) \quad (4)$$

$$\sigma_{yield} = C + P\mu \quad (5)$$

$$\eta_{plastic} = \frac{\sigma_{yield}}{2\dot{\varepsilon}_{II}} \quad (6)$$

$$\eta_{eff} = \min\left(\eta_{ductile}, \eta_{plastic}\right) \quad (7)$$

We consider partial melting of rocks in the models. Partial melting of the solid rock is a function (**Eq. 8**) of temperature and pressure (Schmidt and Poli, 1998), where M is the volumetric melt fraction, $T_{solidus}$ and $T_{liquidus}$ are the solidus and liquids, respectively.

$$M = \begin{cases} 0 & T \le T_{solidus} \\ \dfrac{T - T_{solidus}}{T - T_{liquidus}} & T_{solidus} < T < T_{liquidus} \\ 1 & T \ge T_{liquidus} \end{cases} \quad (8)$$

Model Setup

The initial model setup is shown in **Figure 3**. The dimension of the model box is 7,000 × 2,925 km consisting of 501 × 451

TABLE 1 | Parameters and results of the typical numerical models.

Figure	Initial moho temperature (°C)	Upper crustal thickness (km)	Lower crustal rheological flow law	Results
Figure 4, **Figure 5**, **Figure 8B**, **Figure 9B**	450	25	Mafic granulite	Intra-crustal delamination
Figure 6A, **Figure 8A**, **Figure 9A**	500	25	Felsic granulite	Along-Moho delamination
Figure 6B	600	20	Felsic granulite	Along-Moho delamination with deep depth breakoff
Figure 6C	650	20	Felsic granulite	Along-Moho delamination with shallow depth breakoff
Figure 6D, **Figure 8C**, **Figure 9C**	450	20	Felsic granulite	Continental subduction

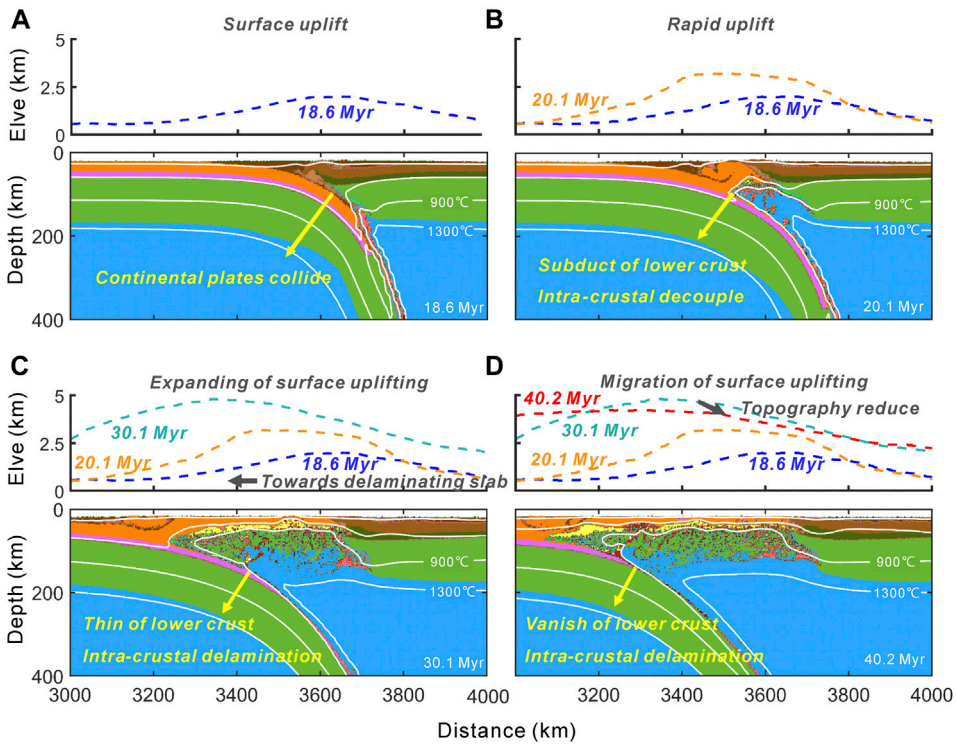

FIGURE 4 | Typical model evolution of intra-crustal delamination. **(A-D)** Snapshots shown by lithology and surface elevation. The main parameters of the continental plates: 25 and 15 km thick upper and lower crust, respectively; mafic granulite of the lower crustal lithology; and 450°C initial Moho temperature.

numerical nodes distributed nonuniformly with the highest resolution in the middle of the model domain. Grid space increases from 4 km in the middle of the model domain to 24 km on the left and right edges horizontally, and increases from 1 km on the top boundary to 12 km on the lower boundary vertically. The velocity boundary condition is free slip on all the boundaries (**Figure 3B**). The top layer is sticky air, underlain by the homogeneous crustal layer and lithospheric mantle layer (**Figure 3A**). Horizontally, the model is divided into three parts (**Figure 3A**): the left continent plate, the middle oceanic plate with a hanging slab nose driving subduction, and the right continent plate. We calculate the initial lithospheric strength (**Figures 3C–E**) using the following parameters, i.e., constant strain rate ($\dot{\varepsilon} = 1 \times 10^{-15}$ s^{-1}), effective friction coefficient (μ = 0.6) and cohesion (C = 0.7 Mpa). The thickness of the upper continental crust may influence model evolution and its effect is systematically tested by varying its thickness (**Figure 3C**). We prescribe the rheology of wet quartzite and dry olivine for the upper crust and the mantle lithosphere, respectively. Regarding the lower crust, varied rock lithology/rheology (i.e., felsic granulite, plagioclase, diabase, and mafic granulite) are tested (**Figure 3D**).

The initial thermal state of the lithosphere is horizontally uniform with zero heat flux across the vertical boundaries. The crustal surface, Moho, and the lithosphere-asthenosphere boundary (LAB) has an initial temperature of 0°C, 450°C, and

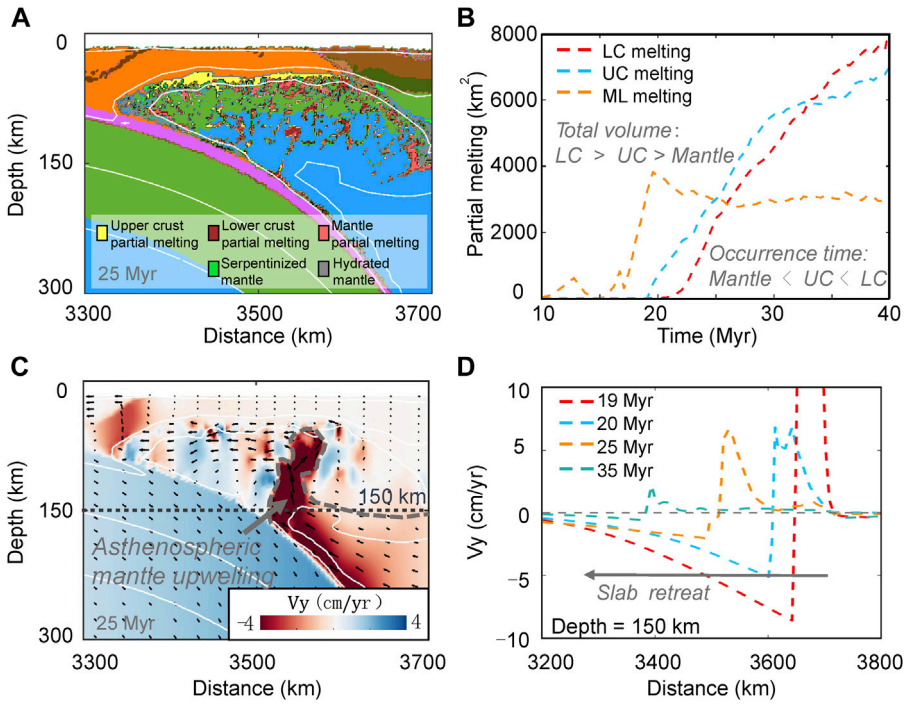

FIGURE 5 | Detailed model evolution of intra-crustal continental delamination. **(A)** Snapshots of model evolution. **(B)** Volume of lithosphere partial melting. **(C)** Snapshots of model velocity for *Y* direction. White line is temperature. Black arrows represent the magnitude and direction of the velocity. **(D)** Velocity for *Y* direction with 150 km depth in different time.

1,300°C, respectively. Temperature increases linearly in the crust and mantle lithosphere. The initial temperature along the base of the oceanic plate is around 1,009°C as a consequence to the linear temperature interpolation. We use linear temperature interpolation for the oceanic plate instead of using half space cooling model mainly because we aim to reduce sensitivity test on oceanic subduction but focus on the following collisional processes. Beneath the LAB, the initial temperature gradient is prescribed as 0.5°C/km. We also test the effect of the Moho temperature on model evolution by varying the initial values (**Figure 3E**; i.e., changing systematically from 300° to 800°C).

MODEL RESULTS

We conducted a series of numerical models with particular attention paid on investigating the effect of intra-crustal decoupling on continental delamination. The effect of various parameters (i.e., the upper crustal thickness, the lower crustal rheology, and the initial Moho temperature) is systematically tested. The model results we use in this paper is summarized in the **Table 1**.

Intra-Crustal Continental Delamination

Intra-crustal continental delamination typically occurs along the interface of the upper and lower crust, affected by intra-crustal strength decoupling, and the detailed model evolution is shown in **Figure 4**. The model evolves driven by oceanic subduction due to the initial hanging slab nose (**Figure 4A**). After a certain time, two continental plates collide, resulting in continental collision and exhumation of the upper crust (**Figure 4B**). Surface elevation increases dramatically as a consequence to the shortening and thickening of the upper crust. The lower crust subducts attached to the lithospheric mantle (**Figure 4B**). Continental delamination occurs along the upper and lower crustal interface, promoted by the mechanical decoupling between the upper and lower crust (**Figure 4C**). The subducted lower crust experiences intensive partial melting (**Figure 4C**). Besides, warm asthenosphere upwells and fills the space caused by continental delamination, which further promotes crustal partial melting beneath the upper crust (**Figures 4C,D**). Surface elevation decreases in the collisional domains and increases to the delaminated continental plate, since the upper crustal thickening is mainly located in the delaminated continental plate.

Intensive crustal and mantle partial melting is formed during the model evolution (**Figure 5A**). The lithospheric mantle first experiences partial melting due to subduction and slab dehydration (**Figure 5B**), followed by the partial melting of the upper crust due to the heating of the upwelling asthenospheric mantle (**Figures 5C,D**). New lithospheric mantle forms underneath the upper crust due to the cooling of the warm asthenospheric mantle (**Figure 5A**). Melting of the lower crust occurs later than that of the upper crust, likely due to high pressure since it subducts attached to lithospheric mantle. Partial melting of the mantle occurs much earlier than that of crust, and decays with time due to solidification (**Figure 5B**).

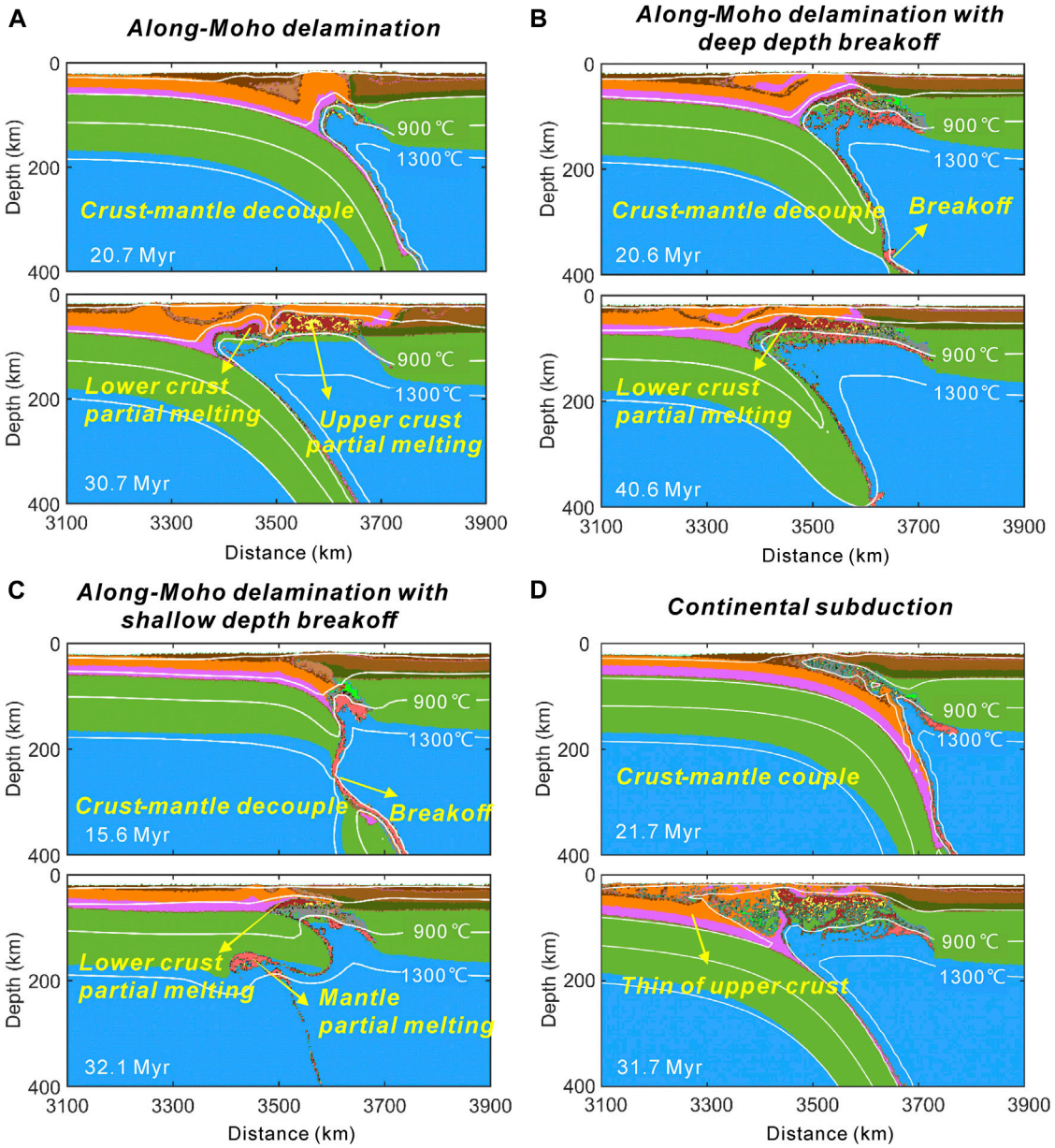

FIGURE 6 | Various types of model evolution. **(A)** Along-Moho continental delamination without slab breakoff. Main parameters used: 25 and 15 km upper and lower crustal thickness, respectively; felsic granulite of the lower crustal lithology; and 500°C initial Moho temperature. **(B–C)** Delamination with deep and shallow slab breakoff. The major changed parameters: equal thickness of 20 km of the upper and lower crust; 600°C **(B)** and 650°C **(C)** initial Moho temperature. **(D)** Continental subduction. The major changed parameters: 20 and 20 km upper and lower crustal thickness, respectively; 450°C initial Moho temperature.

Various Types of Model Evolution

Our model results also reveal the development of along-Moho delamination and continental subduction (**Figure 6**). The along-Moho continental delamination occurs favored by crust-mantle decoupling (e.g., **Figure 6A**), which is a common feature in the models with weak lower crust (due to weak rock lithology or high Moho temperature). In this type of model, subduction of the weak lower crust is retarded by the upwelling of the asthenospheric mantle, and continental delamination occurs along the Moho. As a consequence, the lower crust experience intensive partial melting earlier than that of the upper crust. Slab breakoff often occurs in this type of models mainly due to the decrease of the lithospheric strength, and the deep and shallow slab breakoff modes are recognized (**Figures 6B,C**). With the decrease in lithospheric strength (for instance, increase the initial Moho temperature), slab breakoff tends to occur at the shallow depth. Once slab breakoff happens, the dynamic evolution of continental delamination is significantly inhibited due to the loss of slab pull.

Continental subduction forms in a number of models, featured by the subduction of the entire crust, i.e., both the upper and

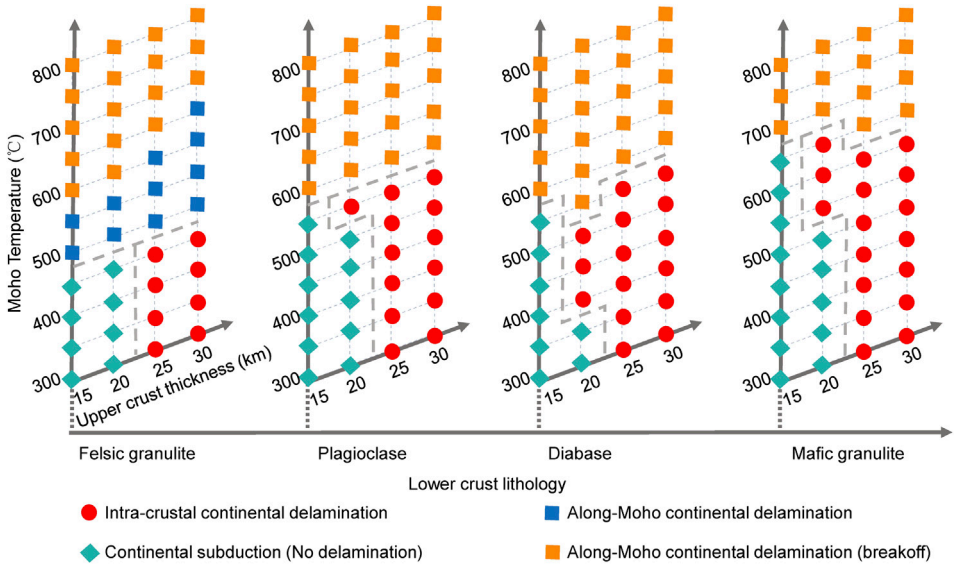

FIGURE 7 | Model results of parameter test. Blue square is along-Moho delamination with slab break off; orange rhombus is continental subduction; green triangle is along-Moho delamination; red circle is intra-crustal delamination. The grey arrow from the left to the right shows the variation of the lower crustal lithology.

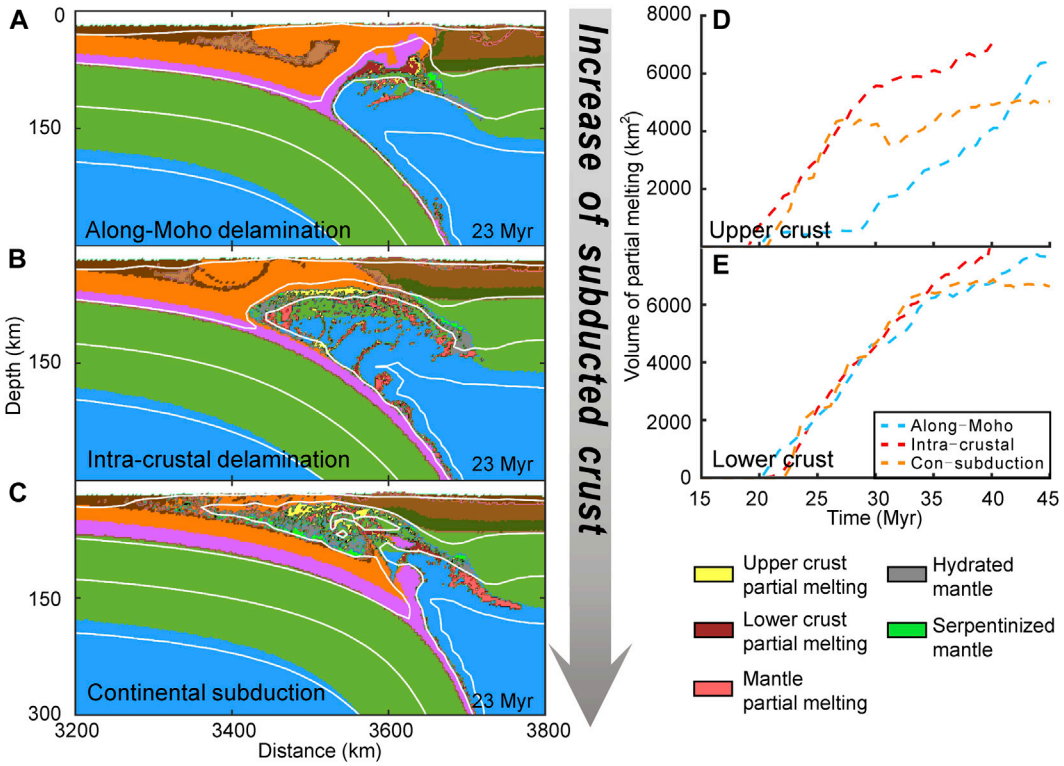

FIGURE 8 | Model comparison of the three different modes. **(A–C)** Model results shown by lithological snapshots indicating the amount of subducted crust (i.e., from no crust subducted to the entire crust subducted). Intra-crustal delamination model from **Figure 4**, along-Moho delamination model from **Figure 6A**, and continental subduction model from **Figure 6D**. **(D–E)** Partial melting of the upper crust and lower crust of the three models.

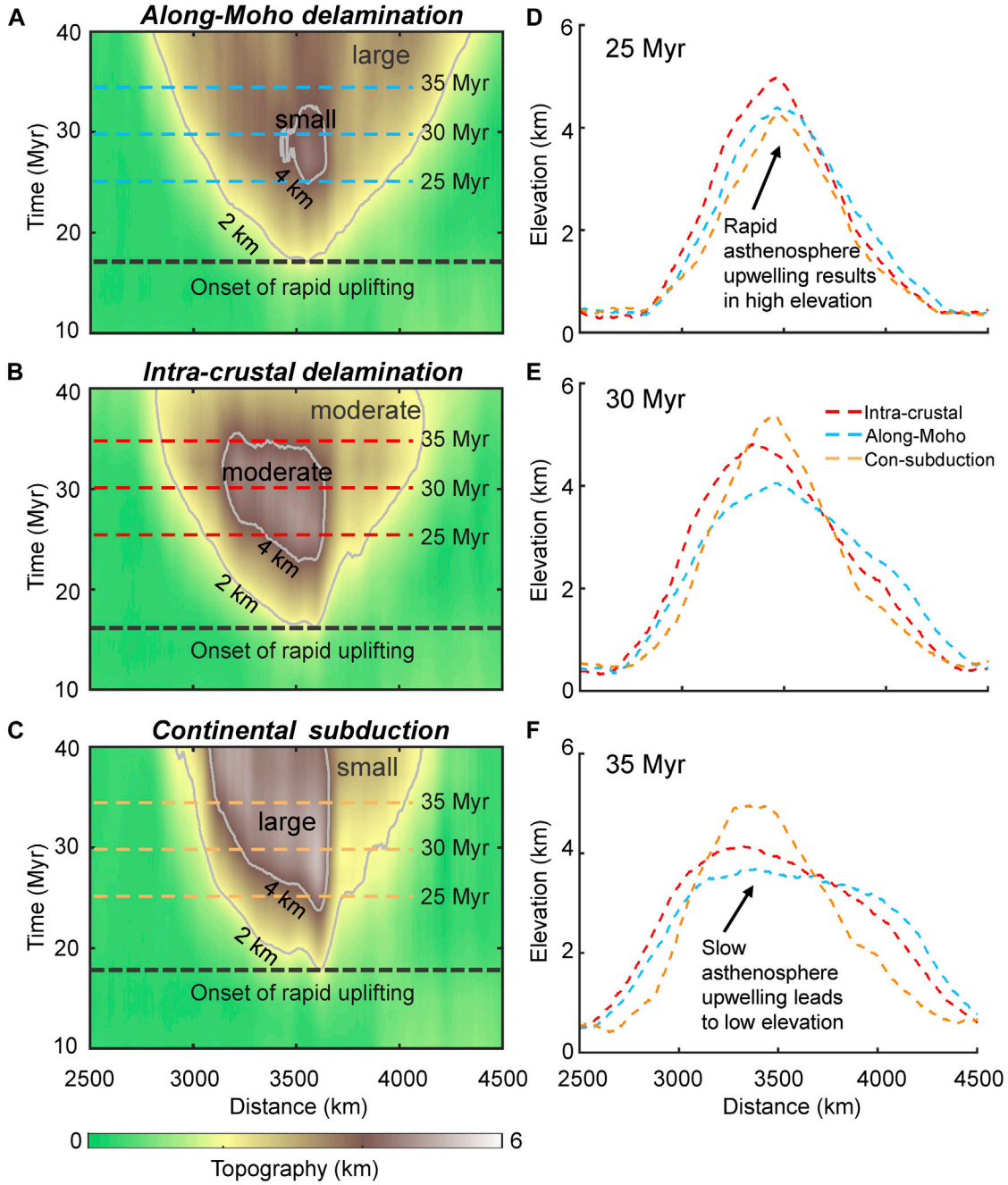

FIGURE 9 | Topography variations of the three models. **(A–C)** Temporal evolution of surface elevation of the three models. **(D–F)** Topography at 25, 30, 35 Myr for Panels **(A–C)**.

lower crust subduct attached to the lithospheric mantle (**Figure 6D**). The development of continental subduction is favored by strong lithospheric coupling i.e., both intra-crustal coupling and crust-mantle coupling (**Figure 6D**). Warm asthenospheric mantle upwells to shallow depth, intruding on top of the upper crust (**Figure 6D**). During continental subduction, the upper crust experiences intensive partial melting while melting of the lower crust is largely inhibited and postponed. Exhumation of crustal rocks is negligible in this model.

Parameter Effects on Intra-Crustal Delamination

The development of intra-crustal delamination is largely promoted by intra-crustal strength decoupling, i.e., the base

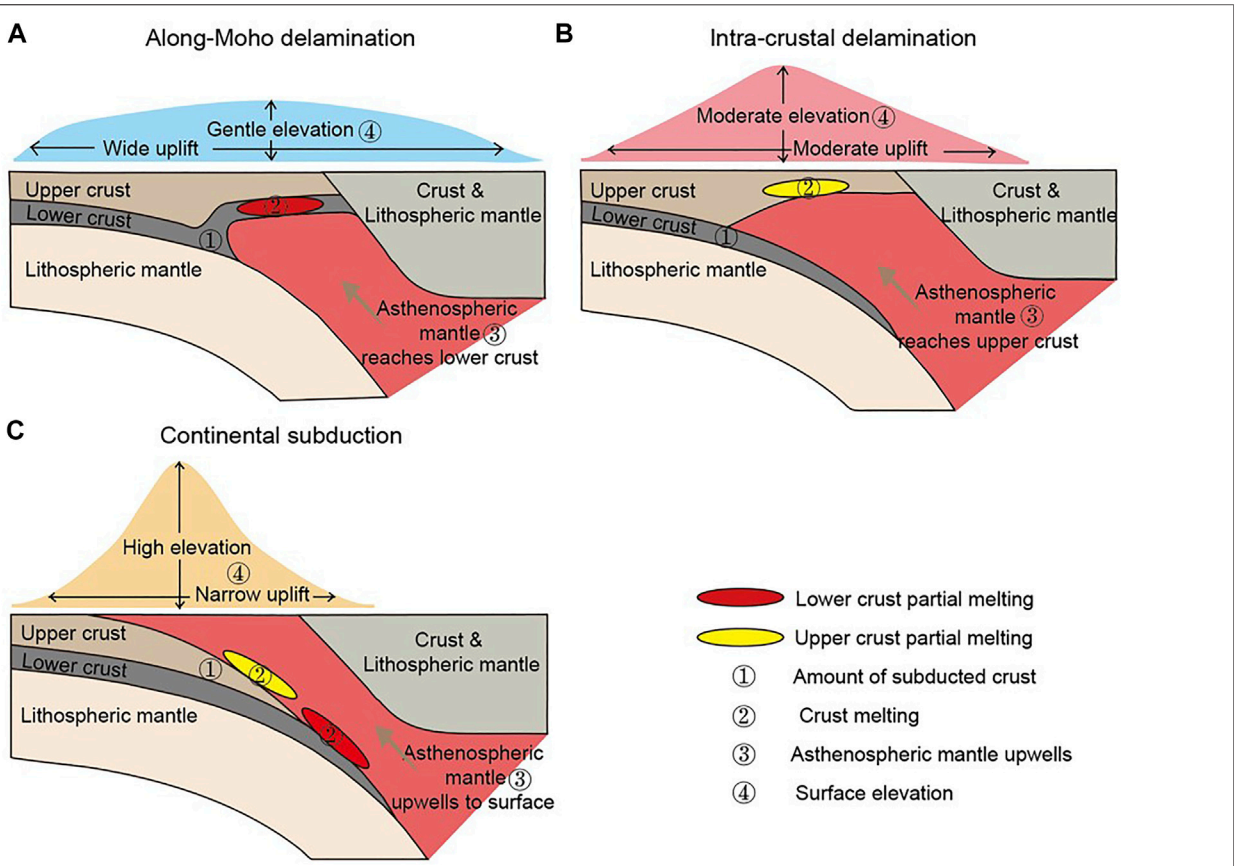

FIGURE 10 | Summarized features of these three types of models. **(A–C)** Along-Moho delamination, intra-crustal delamination and continental subduction models.

of the upper crust is mechanically weak and results in strength drop along the interface between the upper and lower crust. The major parameters affecting intra-crustal delamination are the upper crustal thickness, the lower crustal lithology and the initial Moho temperature (**Figure 7**). 1) Thick upper crust tends to promote the development of intra-crustal delamination, mainly because the lower part of the thick upper crust is mechanically weak and thus promotes intra-crustal strength decoupling. The threshold of the upper crustal thickness affecting the intra-crustal delamination is around 20 km (**Figure 7**). Decrease the upper crustal thickness results in the increase of the intra-crustal coupling, which promotes the formation of continental subduction and along-Moho delamination. 2) The initially prescribed Moho temperature is an important parameter affecting lithospheric thermal structure and rheological layering, which thus influences lithospheric dynamics (Gueydan et al., 2008; Liao et al., 2017). Model results show that initially low Moho temperature promotes the development of intra-crustal delamination. Increase the initial Moho temperature, along-Moho continental delamination becomes the dominant evolution type. Slab breakoff often happens in the along-Moho delamination models, because high initial Moho temperature results in the strength decrease of the subduction slabs, which is consistent with the previous study (Duretz et al., 2011). 3) The lower crustal lithology also affects the intra-crustal delamination. We tested four different lower crustal lithologies (i.e., felsic granulite, plagioclase, diabase, and mafic granulite). The mechanical strength increases gradually from more felsic lithology to more mafic lithology. Model results show that with more mafic lithology (e.g., mafic granulite), intra-crustal delamination occurs in much wider parameter space (**Figure 7**). The main reason is that mechanically stronger lower crust promotes crust-mantle coupling and favors intra-crustal decoupling.

DISCUSSION

Comparison of the Various Model Types

The dynamic evolution of the intra-crustal delamination model is compared to the along-Moho delamination model and the continental subduction model (**Figures 8–10**). The remarkable difference of these three models is the amount of subducted crust (**Figures 8A–C**) that increases from the along-Moho delamination model (i.e., no crust subducted)

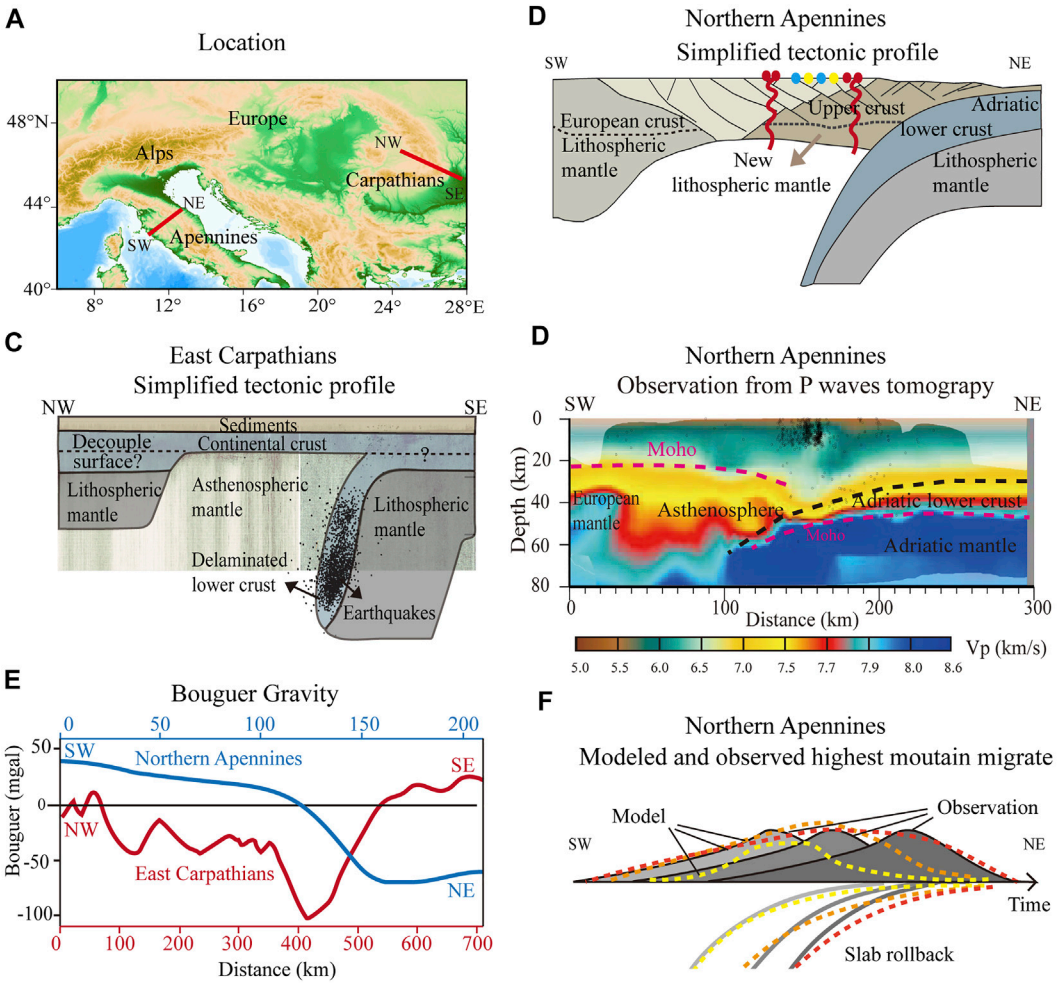

FIGURE 11 | Possible natural examples showing intra-crustal delamination. **(A)** Locations of the Northern Apennines and the East Carpathians. **(B)** Top: Simplified tectonic profile of the Northern Apennines modified from Carminati and Doglioni (2012). The red circles represent the volcanic centers containing mantle-derived magmas, and the yellow and blue circles mark the acid volcanos and plutons produced mostly by crustal anatexis, respectively (Serri et al., 1993). **(C)** Simplified tectonic profile of the East Carpathians. **(D)** *P* wave velocity of the Northern Apennines (Di Stefano et al., 2009). **(E)** Bouguer Gravity of the Northern Apennines (blue line, Carminati and Doglioni, 2012) and the East Carpathians (red line, Sperner et al., 2004). **(F)** Modeled (the colored dashed lines) and observed (the shaded area) topography migration of the Apennines controlled by slab rollback (Galli et al., 2002).

to the intra-crustal delamination model (i.e., the lower crust subducted) and continental subduction model (i.e., the entire crust subducted). As a consequence, the crustal partial melting varies among these models (**Figures 8D,E**). 1) The intra-crustal delamination model experiences the most intensive melting of the upper crust (**Figure 8D**), mainly due to the direct heating of the upwelling asthenospheric mantle along the base of the upper crust (**Figure 8B**). On the contrary, the standard along-Moho delamination model generates very limited upper crustal melting, especially in the early stage (<30 Myr), due to the isolation from the asthensopheric mantle by the lower crust (**Figure 8A**). 2) Lower crustal partial melting is first formed in the along-Moho model, but the intensity of lower crustal melting is quite similar in all these models (**Figure 8E**).

The difference in dynamic evolution of these three types of models is revealed by surface elevation (**Figure 9**). The along-Moho delamination model (**Figure 9A**) is featured by widespread surface uplifting (i.e., the large 2 km surface elevation contour) with gentle elevation (i.e., the small 4 km surface elevation contour). The continental subduction model (**Figure 9C**), however, is marked by concentrated high surface uplifting (i.e., the small 2 km elevation contour but large 4 km elevation contour). These two types of models are the two end-members, and the intra-crustal delamination model (**Figure 9B**) shows the moderate surface uplifting (i.e., both the 2 and 4 km elevation contours). The main reason influencing the surface uplift in these three models is the amount of subducted crust. The entire crust subducts in the continental subduction model, and warm

asthenospheric mantle upwells to near-surface resulting in concentrated high elevation. No crust subducts in the along-Moho delamination model, and warm asthenospheric mantle upwells to Moho depth leading to widespread surface uplifting. The intra-crustal delamination model with only lower crust subducted thus forms moderate surface elevation between the two end-members. The decrease of the highest surface elevation with time (**Figures 9D–F**) is due to the decline of the warm asthenospheric mantle (**Figure 5D**).

The difference of intra-crustal delamination model from the along-Moho delamination model and the continental subduction model can be summarized by **Figure 10**. Firstly, the amount of subducted crust in the intra-crustal delamination model (i.e., the lower crust subducted) is larger than that in the along-Moho delamination model (i.e., no crust subducted) but smaller than the continental subduction model (i.e., the entire crust subducted). Secondly, upper crustal melting is a more common phenomenon in the intra-crustal delamination models than that in the other two models because the warm asthenospheric mantle contacts the upper crust directly. Thirdly, asthenospheric mantle upwells to the upper crustal depth in the intra-crustal delamination model, results in moderate surface elevation compared to the other two models. Thus, the intra-crustal delamination model is a transition mode between the along-Moho delamination model and the continental subduction model in terms of subducted crust, crustal melting, mantle upwelling and surface elevation (**Figure 10**).

Comparison With the Possible Natural Examples

The geological and geophysical observations of the Northern Apennines and the East Carpathians (**Figure 11A**) reveal the possibility of intra-crustal delamination (**Figure 11**). Firstly, the studies using high-resolution tele-seismic tomography and deep seismic reflection data revealed the possibility of intra-crustal delamination in the Northern Apennines and the East Carpathians (**Figures 11B–D**; Piana Agostinetti et al., 2002; Pauselli et al., 2006; Di Stefano et al., 2009; Fillerup et al., 2010; Giacomuzzi et al., 2011; Piana Agostinetti and Faccenna, 2018). In the Northern Apennines, the interpreted geophysical image shows that the Adriatic upper crust atop the mantle wedge and the Adriatic lower crust delaminates attached to the subducting plate (**Figure 11B**). The Adriatic upper crust undergoes intensive deformation featured by the wide-distributed faults (**Figure 11B**; Carminati et al., 2004; Faccenna et al., 2014). Another important feature is the newly formed lithospheric mantle underneath the Adriatic upper crust. The *P* wave velocity structure reveals delamination of the Adrian lower crust, and the low *Vp* anomalies deplict the upwelling of the asthenospheric mantle (**Figure 11D**). Secondly, the geochemistry study revealed metasomatized mantle in the mantle wedge with k-rich melt possibly derived from the subducted Adriatic upper crust (Serri et al., 1993), indicating the possibility of the intra-crustal delamination. Thirdly, the low Bouguer gravity (**Figure 11E**) in the Northern Apennines (Carminati and Doglioni, 2012) and East Carpathians (Sperner et al., 2004) could be affected by lithosphere upwelling as a result from lithosphere delamination. Fourthly, the morphologic study using the data of water divide analyzed the Apennines divide and the highest mountains, and suggested that the highest mountains migrated to the east, consistent with the eastward retreat of the delaminated Apennines slab in the Pliocene and Quaternary (**Figure 11F**; Galli et al., 2002). The above-mentioned features are all captured in our models (e.g., **Figures 4**, **5**, **10**).

CONCLUSION

We study systematically the dynamical evolution of intra-crustal delamination using 2D thermomechanical numeric modeling. Our model results suggest the following conclusions.

(1) Intra-crustal continental delamination is a possible way of continental destruction, facilitated by intra-crustal strength decoupling. The formation of intra-crustal continental delamination is largely promoted by thick upper crust, low Moho temperature and more mafic lower crustal lithology.
(2) Intra-crustal continental delamination differs from the standard along-Moho delamination and continental subduction in terms of the amount of subducted crust, the intense of partial melting and surface elevation.
(3) The possibility of intra-crustal continental delamination is supported by the observations of the Northern Apennines and the East Carpathians.

DATA AVAILABILITY STATEMENT

The datasets presented in this study can be found in online repositories. The names of the repository/repositories and accession number(s) can be found below: http://doi.org/10.5281/zenodo.5030906.

AUTHOR CONTRIBUTIONS

RQ: Conceptualization, Writing—Original Draft, Visualization. JL: Methodology, Writing—Review and Editing, Supervision, Resources, Conceptualization, Project administration. RG: Conceptualization, Supervision, Resources, Project administration.

FUNDING

This research is financially supported by NSFC projects (U1901214, 41974104, 91855208) and Guangdong project 2017ZT07Z066. Numerical simulations were run with the clusters of National Supercomputer Center in Guangzhou (Tianhe-II).

ACKNOWLEDGMENTS

We thank Prof. Taras Gerya for his long-standing guidance on our geodynamical modeling work. Prof. Lun Li, Dr. Hongda Liang and Dr. Xingfu Huang are thanked for their valuable suggestions on this study.

SUPPLEMENTARY MATERIAL

The Supplementary Material for this article can be found online at: https://www.frontiersin.org/articles/10.3389/feart.2022.829300/full#supplementary-material

REFERENCES

Afonso, J. C., and Ranalli, G. (2004). Crustal and Mantle Strengths in continental Lithosphere: Is the Jelly sandwich Model Obsolete. *Tectonophysics* 394, 221–232. doi:10.1016/j.tecto.2004.08.006

Beall, A. P., Moresi, L., and Stern, T. (2017). Dripping or Delamination? A Range of Mechanisms for Removing the Lower Crust or Lithosphere. *Geophys. J. Int.* 210, 671–692. doi:10.1093/gji/ggx202

Bird, P. (1979). Continental Delamination and the Colorado Plateau. *J. Geophys. Res.* 84, 7561–7571. doi:10.1029/JB084iB13p07561

Bird, P. (1978). Initiation of Intracontinental Subduction in the Himalaya. *J. Geophys. Res.* 83, 4975–4987. doi:10.1029/JB083iB10p04975

Bousquet, R., Goffé, B., Henry, P., Le Pichon, X., and Chopin, C. (1997). Kinematic, thermal and Petrological Model of the Central Alps: Lepontine Metamorphism in the Upper Crust and Eclogitisation of the Lower Crust. *Tectonophysics* 273, 105–127. doi:10.1016/S0040-1951(96)00290-9

Burg, J.-P., and Gerya, T. V. (2005). The Role of Viscous Heating in Barrovian Metamorphism of Collisional Orogens: Thermomechanical Models and Application to the Lepontine Dome in the Central Alps. *J. Metamorph Geol.* 23, 75–95. doi:10.1111/j.1525-1314.2005.00563.x

Burov, E. B. (2011). Rheology and Strength of the Lithosphere. *Mar. Pet. Geology.* 28, 1402–1443. doi:10.1016/j.marpetgeo.2011.05.008

Carminati, E., and Doglioni, C. (2012). Alps vs. Apennines: The Paradigm of a Tectonically Asymmetric Earth. *Earth-Science Rev.* 112, 67–96. doi:10.1016/j.earscirev.2012.02.004

Carminati, E., Doglioni, C., and Barba, S. (2004). Reverse Migration of Seismicity on Thrusts and normal Faults. *Earth-Science Rev.* 65, 195–222. doi:10.1016/S0012-8252(03)00083-7

Clauser, C., and Huenges, E. (1995). T*Hermal Conductivity of Rocks and Minerals*., 23.

Di Stefano, R., Kissling, E., Chiarabba, C., Amato, A., and Giardini, D. (2009). Shallow Subduction beneath Italy: Three-Dimensional Images of the Adriatic-European-Tyrrhenian Lithosphere System Based on High-qualityPwave Arrival Times. *J. Geophys. Res.* 114, B05305. doi:10.1029/2008JB005641

Dong, X., Li, W., Lu, Z., Huang, X., and Gao, R. (2020). Seismic Reflection Imaging of Crustal Deformation within the Eastern Yarlung-Zangbo Suture Zone. *Tectonophysics* 780, 228395. doi:10.1016/j.tecto.2020.228395

Duretz, T., Gerya, T. V., and May, D. A. (2011). Numerical Modelling of Spontaneous Slab Breakoff and Subsequent Topographic Response. *Tectonophysics* 502, 244–256. doi:10.1016/j.tecto.2010.05.024

Faccenda, M., Minelli, G., and Gerya, T. V. (2009). Coupled and Decoupled Regimes of continental Collision: Numerical Modeling. *Earth Planet. Sci. Lett.* 278, 337–349. doi:10.1016/j.epsl.2008.12.021

Faccenna, C., Becker, T. W., Miller, M. S., Serpelloni, E., and Willett, S. D. (2014). Isostasy, Dynamic Topography, and the Elevation of the Apennines of Italy. *Earth Planet. Sci. Lett.* 407, 163–174. doi:10.1016/j.epsl.2014.09.027

Fillerup, M. A., Knapp, J. H., Knapp, C. C., and Raileanu, V. (2010). Mantle Earthquakes in the Absence of Subduction? Continental Delamination in the Romanian Carpathians. *Lithosphere* 2, 333–340. doi:10.1130/L102.1

Galli, C. S., Torrini, A., Doglioni, C., and Scrocca, D. (2002). Divide and Highest Mountains vs Subduction in the Apennines. *Studi Geol. Cam.* 1, 143–145. http://193.204.8.201:8080/jspui/handle/1336/822.

Gao, R., Lu, Z., Klemperer, S. L., Wang, H., Dong, S., Li, W., et al. (2016). Crustal-scale Duplexing beneath the Yarlung Zangbo Suture in the Western Himalaya. *Nat. Geosci* 9, 555–560. doi:10.1038/ngeo2730

Gerya, T. V., and Yuen, D. A. (2003). Characteristics-based Marker-In-Cell Method with Conservative Finite-Differences Schemes for Modeling Geological Flows with Strongly Variable Transport Properties. *Phys. Earth Planet. Interiors* 140, 293–318. doi:10.1016/j.pepi.2003.09.006

Gerya, T. V., and Yuen, D. A. (2007). Robust Characteristics Method for Modelling Multiphase Visco-Elasto-Plastic Thermo-Mechanical Problems. *Phys. Earth Planet. Interiors* 163, 83–105. doi:10.1016/j.pepi.2007.04.015

Giacomuzzi, G., Chiarabba, C., and De Gori, P. (2011). Linking the Alps and Apennines Subduction Systems: New Constraints Revealed by High-Resolution Teleseismic Tomography. *Earth Planet. Sci. Lett.* 301, 531–543. doi:10.1016/j.epsl.2010.11.033

Göğüş, O. H., Pysklywec, R. N., Corbi, F., and Faccenna, C. (2011). The Surface Tectonics of Mantle Lithosphere Delamination Following Ocean Lithosphere Subduction: Insights from Physical-Scaled Analogue Experiments. *Geochem. Geophys. Geosyst.* 12. doi:10.1029/2010GC003430

Göğüş, O. H., Pysklywec, R. N., and Faccenna, C. (2016). Postcollisional Lithospheric Evolution of the Southeast Carpathians: Comparison of Geodynamical Models and Observations. *Tectonics* 35, 1205–1224. doi:10.1002/2015TC004096

Göğüş, O. H., and Pysklywec, R. N. (2008). Mantle Lithosphere Delamination Driving Plateau Uplift and Synconvergent Extension in Eastern Anatolia. *Geol* 36, 723. doi:10.1130/G24982A.1

Göğüş, O. H., and Ueda, K. (2018). Peeling Back the Lithosphere: Controlling Parameters, Surface Expressions and the Future Directions in Delamination Modeling. *J. Geodynamics* 117, 21–40. doi:10.1016/j.jog.2018.03.003

Gueydan, F., Morency, C., and Brun, J.-P. (2008). Continental Rifting as a Function of Lithosphere Mantle Strength. *Tectonophysics* 460, 83–93. doi:10.1016/j.tecto.2008.08.012

Guo, X., Li, W., Gao, R., Xu, X., Li, H., Huang, X., et al. (2017). Nonuniform Subduction of the Indian Crust beneath the Himalayas. *Sci. Rep.* 7, 12497. doi:10.1038/s41598-017-12908-0

Kay, R. W., and Mahlburg Kay, S. (1993). Delamination and Delamination Magmatism. *Tectonophysics* 219, 177–189. doi:10.1016/0040-1951(93)90295-U

Kirby, S. H., and Kronenberg, A. K. (1987). Rheology of the Lithosphere: Selected Topics. *Rev. Geophys.* 25, 1219. doi:10.1029/RG025i006p01219

Krystopowicz, N. J., and Currie, C. A. (2013). Crustal Eclogitization and Lithosphere Delamination in Orogens. *Earth Planet. Sci. Lett.* 361, 195–207. doi:10.1016/j.epsl.2012.09.056

Li, Z.-H., Liu, M., and Gerya, T. (2016). Lithosphere Delamination in continental Collisional Orogens: A Systematic Numerical Study. *J. Geophys. Res.* 26.

Liang, H., Jin, S., Wei, W., Gao, R., Ye, G., Zhang, L., et al. (2018). Lithospheric Electrical Structure of the Middle Lhasa Terrane in the South Tibetan Plateau. *Tectonophysics* 731-732, 95–103. doi:10.1016/j.tecto.2018.01.020

Liao, J., Gerya, T., and Malusà, M. G. (2018). 3D Modeling of Crustal Shortening Influenced by Along-Strike Lithological Changes: Implications for continental Collision in the Western and Central Alps. *Tectonophysics* 746, 425–438. doi:10.1016/j.tecto.2018.01.031

Liao, J., Gerya, T., Thielmann, M., Webb, A. A. G., Kufner, S.-K., and Yin, A. (2017). 3D Geodynamic Models for the Development of Opposing continental Subduction Zones: The Hindu Kush-Pamir Example. *Earth Planet. Sci. Lett.* 480, 133–146. doi:10.1016/j.epsl.2017.10.005

Magni, V., Faccenna, C., van Hunen, J., and Funiciello, F. (2013). Delamination vs. Break-Off: the Fate of continental Collision. *Geophys. Res. Lett.* 40, 285–289. doi:10.1002/grl.50090

Pauselli, C., Barchi, M. R., Federico, C., Magnani, M. B., and Minelli, G. (2006). The Crustal Structure of the Northern Apennines (Central Italy): An Insight by the Crop03 Seismic Line. *Am. J. Sci.* 306, 428–450. doi:10.2475/06.2006.02

Piana Agostinetti, N., and Faccenna, C. (2018). Deep Structure of Northern Apennines Subduction Orogen (Italy) as Revealed by a Joint Interpretation of Passive and Active Seismic Data. *Geophys. Res. Lett.* 45, 4017–4024. doi:10.1029/2018GL077640

Piana Agostinetti, N., Lucente, F. P., Selvaggi, G., and Di Bona, M. (2002). Crustal Structure and Moho Geometry beneath the Northern Apennines (Italy). *Geophys. Res. Lett.* 29, 60. doi:10.1029/2002GL015109

Schmid, S. M., Kissling, E., Diehl, T., van Hinsbergen, D. J. J., and Molli, G. (2017). Ivrea Mantle Wedge, Arc of the Western Alps, and Kinematic Evolution of the Alps-Apennines Orogenic System. *Swiss J. Geosci.* 110, 581–612. doi:10.1007/s00015-016-0237-0

Schmidt, M. W., and Poli, S. (1998). Experimentally Based Water Budgets for Dehydrating Slabs and Consequences for Arc Magma Generation. *Earth Planet. Sci. Lett.* 163, 361–379. doi:10.1016/S0012-821X(98)00142-3

Schneider, F. M. (2013). Seismic Imaging of Subducting continental Lower Crust beneath the Pamir. *Earth Planet. Sci. Lett.* 12. doi:10.1016/j.epsl.2013.05.015

Schneider, F. M., Yuan, X., Schurr, B., Mechie, J., Sippl, C., Kufner, S. K., et al. (2019). The Crust in the Pamir: Insights from Receiver Functions. *J. Geophys. Res. Solid Earth* 124, 9313–9331. doi:10.1029/2019JB017765

Serri, G., Innocenti, F., and Manetti, P. (1993). Geochemical and Petrological Evidence of the Subduction of Delaminated Adriatic continental Lithosphere in the Genesis of the Neogene-Quaternary Magmatism of central Italy. *Tectonophysics* 223, 117–147. doi:10.1016/0040-1951(93)90161-C

Sperner, B., Ioane, D., and Lillie, R. J. (2004). Slab Behaviour and its Surface Expression: New Insights from Gravity Modelling in the SE-Carpathians. *Tectonophysics* 382, 51–84. doi:10.1016/j.tecto.2003.12.008

Thurner, S., Palomeras, I., Levander, A., Carbonell, R., and Lee, C.-T. (2014). Ongoing Lithospheric Removal in the Western Mediterranean: Evidence from Ps Receiver Functions and Thermobarometry of Neogene Basalts (PICASSO Project). *Geochem. Geophys. Geosyst.* 15, 1113–1127. doi:10.1002/2013GC005124

Vogt, K., Matenco, L., and Cloetingh, S. (2017). Crustal Mechanics Control the Geometry of Mountain Belts. Insights from Numerical Modelling. *Earth Planet. Sci. Lett.* 460, 12–21. doi:10.1016/j.epsl.2016.11.016

Vogt, K., Willingshofer, E., Matenco, L., Sokoutis, D., Gerya, T., and Cloetingh, S. (2018). The Role of Lateral Strength Contrasts in Orogenesis: A 2D Numerical Study. *Tectonophysics* 746, 549–561. doi:10.1016/j.tecto.2017.08.010

Wang, Z., Kusky, T. M., and Capitanio, F. A. (2018). On the Role of Lower Crust and Midlithosphere Discontinuity for Cratonic Lithosphere Delamination and Recycling. *Geophys. Res. Lett.* 45, 7425–7433. doi:10.1029/2017GL076948

Wang, Z., and Kusky, T. M. (2019). The Importance of a Weak Mid-lithospheric Layer on the Evolution of the Cratonic Lithosphere. *Earth-Science Rev.* 190, 557–569. doi:10.1016/j.earscirev.2019.02.010

Wilks, K. R., and Carter, N. L. (1990). Rheology of Some continental Lower Crustal Rocks. *Tectonophysics* 182, 57–77. doi:10.1016/0040-1951(90)90342-6

Conflict of Interest: The authors declare that the research was conducted in the absence of any commercial or financial relationships that could be construed as a potential conflict of interest.

Publisher's Note: All claims expressed in this article are solely those of the authors and do not necessarily represent those of their affiliated organizations, or those of the publisher, the editors and the reviewers. Any product that may be evaluated in this article, or claim that may be made by its manufacturer, is not guaranteed or endorsed by the publisher.